International Journal of Heat and Fluid Flow 29 (2008) 1504–1511

Contents lists available at ScienceDirect

International Journal of Heat and Fluid Flow

journal homepage: www.elsevier.com/locate/ijhff

Investigation of heat transfer between a horizontal tube and gas–solid fluidized bed

Nima Masoumifard, Navid Mostoufi *, Ali-Asghar Hamidi, Rahmat Sotudeh-Gharebagh

Multiphase Systems Research Laboratory, Department of Chemical Engineering, University of Tehran, P.O. Box 11155-4563, Tehran, Iran

ARTICLE INFO

Article history:
Received 22 March 2008
Received in revised form 14 June 2008
Accepted 26 June 2008
Available online 12 August 2008

Keywords:
Fluidized bed
Heat transfer coefficient
Horizontal tube
Temperature penetration depth

ABSTRACT

Experiments have been carried out in a fluidized bed in order to verify the influence of the axial position, particle diameter and the superficial gas velocity on the heat transfer coefficient from a small horizontal tube (D_t = 8 mm) immersed in the fluidized bed. The solid particles used were 280, 490 and 750 μm diameter sand particles, fluidized by air. The experimental results showed that the heat transfer coefficient is increased with increasing the gas velocity, up to a maximum, and then decreases with a slight slope. The heat transfer coefficient was found to decrease by increasing the particle size. The probe position had less influence on the heat transfer coefficients. In order to predict the heat transfer coefficient from the fluidized bed to a horizontally immersed tube, a cluster based model has been proposed. The model predictions were compared with the experimental data of this work as well as those from the literature in a wide range of operating conditions. A close agreement was found between the model predictions and the experimental findings.

1. Introduction

Fluidized beds are widely used in heat recovery processes because of their ability in achieving intense heat transfer and providing uniform temperature within the bed. One of the most efficient methods of heat recovery from the fluidized bed is utilizing horizontally immersed tubes. The heat transfer in a fluidized bed between an immersed tube and the bed is extremely high due to vigorous contact of solid particles with the surface. The heat transfer to horizontal tubes immersed in a fluidized bed has been extensively investigated over the last several decades as summarized by Saxena (1989).

Khan and Turton (1992), Karamavruc and Clark (1996) and Al-Busoul and Abu-Ein (2003) studied the influence of the superficial gas velocity, particle diameter, angular position around the tube and type of solid particles on the heat transfer inside the fluidized bed with an immersed tube. They observed an increase of the heat transfer coefficient with the increase in the superficial gas velocity and with the decrease of particle diameter. Kim et al. (2003) determined the heat transfer and bubble characteristics in the fluidized bed with an immersed horizontal tube bundle and showed that the average heat transfer coefficient is increased with increasing the gas velocity towards a maximum value and then decreases subsequently. Rasouli et al. (2005) studied the effect of annular fins on the heat transfer of a horizontally immersed tube in a bubbling fluidized bed. They observed that heat transfer coefficient is decreased with the use of fins while the total heat transfer coefficient rises as a result of greater surface area. Most recent investigations on heat transfer between horizontally immersed tube and fluidized bed have focused on the larger tube, i.e., $D_t > 2.5$ cm (Khan and Turton, 1992; Karamavruc and Clark, 1996; Li et al., 1993). Nevertheless, few attempts have been reported investigating the heat transfer from horizontal tubes in the size range of 1–8 mm (Friedman et al., 2006). In recent years, fluidized bed heat treating furnaces fired by natural gas have become increasingly popular, particularly in the steel wire manufacturing industry. These fluidized beds use small diameter wires, i.e., $D_t < 10$ mm.

In order to design of industrial fluidized bed heat exchangers, reliable heat transfer models are needed allowing reproduction of the behavior of the process. Many theoretical models have been proposed to estimate the heat transfer coefficient between the immersed tubes and fluidized beds (Saxena, 1989; Pence et al., 1994; Mickley and Fairbanks, 1955; Ozkaynak and Chen, 1980; Gelperin et al., 1969; Botterill, 1986; Baskakov et al., 1973). The variety of conflicting models and correlations for the heat transfer coefficient in fluidized bed applications imply that there is a need for a fundamental understanding of the heat transfer mechanism. One of the oldest and the most widely accepted model is the packet renewal model proposed by Mickley and Fairbanks (1955) and Ozkaynak and Chen (1980). In this model, as in many other models, the residence time of the packets at the heat transfer surface is assumed to govern the heat transfer process. During the emulsion phase contact with the heat exchanging surface, the heat transfer rate is decreased with time due to the effect of the increase of the temperature penetration depth, as can be envisaged in a semi-infinite solid. According to such an approach, the average heat transfer rate

* Corresponding author. Fax: +98 21 6646 1024.
E-mail address: mostoufi@ut.ac.ir (N. Mostoufi).

0142-727X/$ - see front matter © 2008 Elsevier Inc. All rights reserved.
doi:10.1016/j.ijheatfluidflow.2008.06.004

Nomenclature

A	1-(projected heater area/bed area)
A_h	surface area of horizontal tube (m^2)
Bi	Biot number ($h_g d_c/k_c$)
C_c	specific heat of cluster ($J\,kg^{-1}\,K^{-1}$)
C_g	specific heat of gas ($J\,kg^{-1}\,K^{-1}$)
C_s	specific heat of solid particles ($J\,kg^{-1}\,K^{-1}$)
D_{bed}	bed diameter (m)
d_c	cluster diameter (m)
d_p	particle diameter (m)
D_t	diameter of the horizontal tube (m)
f	fraction of wall surface covered by bubbles
g	acceleration due to gravity (ms^{-2})
H_{bed}	bed height (m)
$\overline{h}_c$	time-averaged convective heat transfer coefficient ($W\,m^{-2}\,K^{-1}$)
h_{cc}	instantaneous cluster convective heat transfer coefficient ($W\,m^{-2}\,K^{-1}$)
$\overline{h}_{cc}$	time-averaged cluster convective heat transfer coefficient ($W\,m^{-2}\,K^{-1}$)
h_{gc}	gas convective heat transfer coefficient ($W\,m^{-2}\,K^{-1}$)
I	electric current (A)
k_c	thermal conductivity of cluster ($W\,m^{-1}\,K^{-1}$)
k_g	thermal conductivity of gas ($W\,m^{-1}\,K^{-1}$)
k_s	thermal conductivity of solid particles ($W\,m^{-1}\,K^{-1}$)
m	parameter used in Eqs. (6), (12) and (15)
Pr	Prandtl number ($C_c\,\mu/k_c$)
q''	constant heat flux ($W\,m^{-2}$)
$R_{cluster}$	thermal resistance of cluster ($W^{-1}\,m^2\,K$)
R_{gap}	thermal resistance of gas gap ($W^{-1}\,m^2\,K$)
$\widehat{S}_i$	statistical parameter
t	time (s)
T_b	bed temperature (°C)
T_c	cluster temperature (°C)
T_s	probe surface temperature (°C)
t_0	penetration time of the applied heat flux to the other side of the cluster (s)
U_0	superficial gas velocity ($m\,s^{-1}$)
U_c	transition velocity between bubbling and turbulent fluidization regimes ($m\,s^{-1}$)
U_{mf}	minimum fluidization velocity ($m\,s^{-1}$)
V	electric voltage (V)

Greek symbols

α_c	heat diffusivity of cluster ($m^2\,s^{-1}$)
δ	gas gap thickness (m)
ε_c	voidage of cluster
ε_{iu}	error in response i and event u
ε_{mf}	voidage at minimum fluidizing state
$\pi(M_i\|Y)$	discrimination probability of model M_i
ρ_c	cluster density ($kg\,m^{-3}$)
ρ_g	gas density ($kg\,m^{-3}$)
ρ_s	particle density ($kg\,m^{-3}$)
τ	cluster contact time at the wall (s)
$\tau(t)$	penetration depth of temperature (m)
θ	angular position around the tube, measured counterclockwise from the lateral side of the tube

of the emulsion phase depends on the contact time of the emulsion phase. Karimipour et al. (2007) suggested a new model according to the cluster based approach (CBA) and surface renewal theory for the cluster convective component of total heat transfer coefficient. They proposed two different heat transfer coefficients for partial and total heat penetration steps, considering the time needed for the diffusion of heat into the clusters once in contact with the wall.

In the present study, experiments were performed to measure the heat transfer coefficient between the bed and a small horizontal tube over a wide range of superficial gas velocities, covering both bubbling and turbulent regimes of fluidization. The effects of probe distance from the distributor and particle size on the heat transfer coefficient were also investigated. A model is proposed to predict the overall heat transfer coefficients in the bed of small particles at various gas velocity and particle properties based on the cluster renewal approach with the inclusion of the angle dependent correlation for the gas gap thickness.

2. Experimental study

Experiments were carried out in a fluidized bed of transparent plexiglas cylinder of 2 m height and 15 cm inner diameter as shown in Fig. 1. The solid particles used in this study were sand with mean diameters of 280, 490 and 750 μm with the properties listed in Table 1. U_c is a characterization velocity for transition from the bubbling regime to the turbulent regime, and calculated from Cai et al. (1989) at temperature of 30 °C. The fluidizing air was supplied by an air compressor and its flow was measured by calibrated rotameters.

The heat transfer probe used in this study is shown in Fig. 2. The probe (8 mm OD) was made of a copper tube (70 mm-long) in

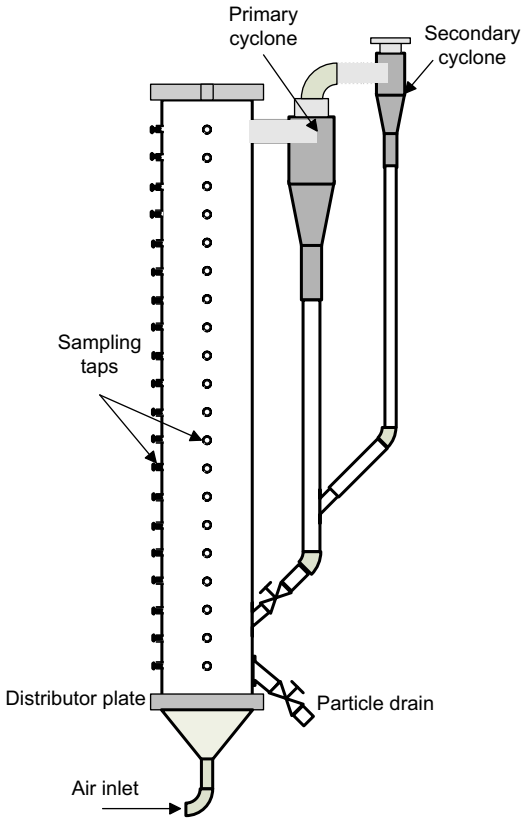

Fig. 1. Schematics of the cold model circulating fluidized bed.

Table 1
Summary of experimental conditions in the present and previous studies (sand particles)

Reference	D_t (mm)	U_0 (m/s)	U_c (m/s)	d_p (μm)	ρ_s (kg m^{-3})	U_{mf} (m/s)
Present study	8	U_{mf}–1.16	1.04	280	2640	0.052
			1.29	490	2640	0.15
			1.52	750	2640	0.42
Friedman et al. (2006)	3.12	(0.5–10)U_{mf}	0.92	203		~0.03
	7.94					
Kim et al. (2003)	25	0.03–0.18	0.98	240	2582	0.048
Rasouli et al.(2005)	15	0.08–0.25	0.926	200	2660	0.062
			1.09	307	2720	0.082
Grewal and Saxena (1983)	12.7	0.06–0.45	1.235	259 (Alumina)	4015	0.104
	12.7	0.28–0.54	1.318	504	2670	
Sunderesan and Clark (1995)	50	0.155–0.202	1.12	317	2749	0.084

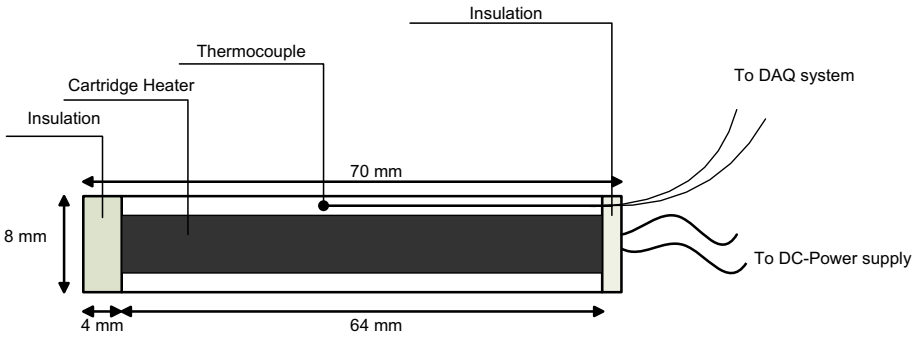

Fig. 2. Schematics of the heat transfer probe.

which a resistance heater (6.5 mm-OD, 64 mm-long) was placed at the center of the tube. Both sides of the probe were insulated to minimize the axial heat loss. The desired power applied to the heater of the probe was controlled by a variable DC power supply. The supplied heat flux was determined by measuring voltage and current of the electric power supplier. A J-type thermocouple (Iron–Constantan) with a bead of 0.12 mm-OD was embedded in the copper tube to monitor the instantaneous surface temperature. During experiments, the probe was horizontally placed at different axial positions in the dense bed. Temperature signals from the thermocouple were amplified and sent via an A/D converter to a computer for recording. The sampling frequency of the signals was 1000 Hz and the total sampling time at each experimental condition was 20 s. The bed temperature was measured by a PT100 type RTD sensor which was installed approximately 50 mm away from the probe.

The superficial air velocity (U_0) was varied in the range of U_{mf} to 1.20 m/s. The measurements of the heat transfer coefficient at any condition were repeated 3 times. With the assumption of minimal heat losses through the insulated ends, the time-averaged local heat transfer coefficient was determined as follows:

$$h = \frac{IV}{A_h(T_s - T_b)} \tag{1}$$

3. Model development

Heat transfer to/from an immersed surface in a fluidized bed at low temperature (<600 °C) consists of two mechanisms: gas convection and particle convection. At high temperatures, the radiant component of the heat transfer becomes important. In the present work, it is assumed that all the particles move as clusters in the bed. Therefore, the average convective heat transfer coefficient could be divided into a convective heat transfer coefficient of the clusters $\overline{h}_{cc}$ on the cluster-covered surface and a gas convective heat transfer coefficient h_{gc} on the uncovered surface:

$$\overline{h}_c = (1-f)\overline{h}_{cc} + (f)h_{gc} \tag{2}$$

The gas convective component of the overall heat transfer coefficient, h_{gc},is usually small, but could be important when there is (i) higher operating pressures than atmospheric, (ii) dilute phase fluidization (high gas velocity), (iii) gas velocities near minimum fluidization, (iv) surface geometries that result in high voidages or stagnant particles and (v) large particle fluidization. These conditions necessitate the inclusion of the gas convective heat transfer. The gas convective heat transfer coefficient h_{gc} could be obtained from (Baskakov et al., 1973):

$$h_{gc} = 0.009\left(\frac{k_g}{d_p}\right)Ar^{0.5}Pr^{0.33} \tag{3}$$

Although this correlation is independent of tube diameter, it has been accepted by many researchers as a good estimate of the gas convective component over a wide range of fluidizing conditions (Modrak, 1979; Glickeman and Decker, 1980). In addition, this expression is not affected by changes in the length of the heat transfer surface, thus, it has been used in this work for estimating the gas convective heat transfer.

The particle/cluster convection component is generally considered to be the most significant mechanism of heat transfer in fluidized beds of small particles operating at or near atmospheric pressure and at relatively low temperatures due to the large heat capacity of solids. There have been two basic approaches underlying the development of useful mathematical models which consider particle convection from the basis of penetration theory.

Both concepts use a two-phase description of the system but approach the characteristics and functions of the phases differently. The first approach models the transient heat conduction for single particles residing at the heat transfer surface where the bed consists of two phases; a continuous gas phase and a discrete solid phase. This approach has resulted in the development of particle based models (Botterill, 1970). Formation of packets of particles (or clusters) from individual solid particles is a major characteristic of the fluidized bed. The transient conduction occurs between a cluster swept up to the wall by bubbles, a stirrer, or by flowing of the particles over the surface. This approach has resulted to packet renewal model or cluster renewal model (Mickley and Fairbanks, 1955), and was also adopted in this work. Based on the experimental findings of Horio and Kuroki (1994), in which they used an imaging technique for detecting the clusters, the shape of clusters is parabola or horseshoe in the downward movement and having a thin tail in upward motion. In order to simplify the mathematical formulation of heat transfer in the present study, the shape of clusters was assumed to be cuboid when contacting the wall.

According to Karimipour et al. (2007), the entire process of heat transfer could be divided into two time periods. Let t_0 be the time needed for the heat effect to completely penetrate into the cluster, from its wall side to the bulk side. This time could be estimated from (Karimipour et al., 2007):

$$t_0 = \frac{d_c^2}{6\alpha_c} \tag{4}$$

In the first period, $0 \leqslant t < t_0$, the heat flux is diffusing inside the cluster but has not reached the other side of the cluster. When the first period is finished, $t \geqslant t_0$, the heat flux has crossed the cluster completely. The second period lasts until the end of the contact time of the cluster with the wall. The residence time of the clusters at the surface is terminated as they are replaced by other clusters with bubble-generated circulation patterns within the bed. Karimipour et al. (2007) considered the process of heat transfer between the cluster and the wall in two above mentioned periods. They showed that the instantaneous heat transfer coefficient in these penetration periods is given by

– For partial penetration period:

$$\overline{h}_{cc} = \frac{1}{R_{cluster}} = \frac{1}{\sqrt{\frac{1.5t}{k_c\rho_c c_c}}} \tag{5}$$

– For total penetration period:

$$\overline{h}_{cc} = \frac{1}{R_{cluster}} = \frac{k_c}{d_c}\frac{1}{\frac{1}{2} + \left(\frac{1}{2} + \frac{1}{Bi}\right)\left\{1 - \exp\left[-\frac{m(t-t_0)}{1+\frac{Bi}{3}}\right]\right\}} \tag{6}$$

where

$$m = \frac{h_{gc}}{\rho_c c_c d_c} \tag{7}$$

One problem in the above formulae is that the heat transfer coefficient predicted by Eq. (5) will approach infinity as the contact time approaches zero, which is not physically realistic. In order to overcome this shortcoming, a thermal resistance between the wall and the cluster, in the form of a gas film, was considered in the present model. The weight of evidence also confirmed the existence of this thermal resistance in the form of a gas gap (Kubie and Broughton, 1975; Baskakov, 1964; Xavier and Davidson, 1978; Gabor, 1970; Decker and Glicksman, 1986; Botterill, 1970; Koppel et al., 1970). Figs. 3a and 3b represent the model concepts based on two heat penetration periods with respect to time, i.e., partial heat penetration and total heat penetration periods. In the case of partial heat penetration, the heat flux applied to the wall side of the cluster has not reached its bed-side, as shown in Fig. 3a. When the heat penetration depth is equal to the thickness of the clusters, the heat flux crosses the cluster and the temperature of its bed-side would differ from the bed temperature. This situation is shown in Fig. 3b. By applying the one dimensional energy balance on a differential element in the gas gap shown in Figs. 3a and 3b at steady state condition, the contact resistance between the cluster and the surface could be obtained as:

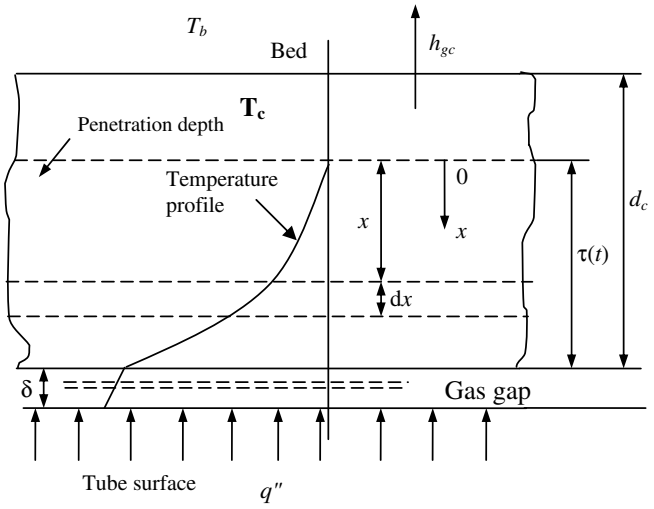

Fig. 3a. Penetration depth of the temperature in (a) partial heat penetration time domain (b) total heat penetration depth.

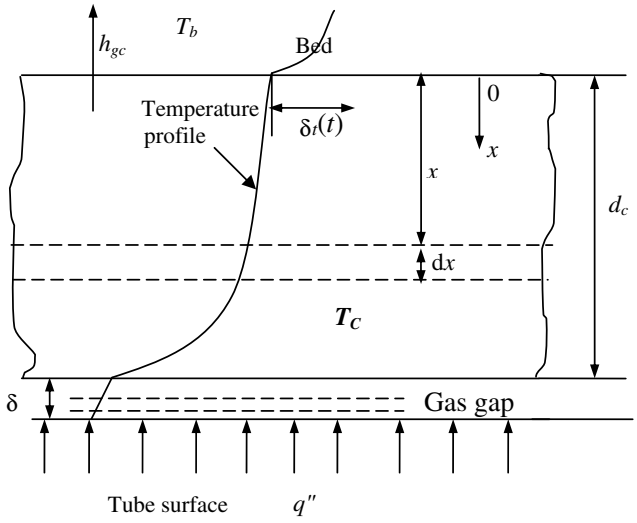

Fig. 3b. Differential systems of heat transfer in (b) total heat penetration depth.

$$R_{gap} = \frac{\delta}{k_g} \tag{8}$$

Huang and Levy (2004) showed, by the use of an instrumented tube, that the gas gap thickness (δ) is a strong function of circumferential position around the horizontal tube. They showed that the gap thickness has a maximum value at the lateral sides of the probe ($\theta = 0^\circ$) and is decreased by moving to the top and bottom sides of the probe ($\theta = +90^\circ$ and -90°, respectively). They also showed that the gas gap thickness is a function of the particle size. According to their experimental findings, the following correlation was

proposed in the present work for the calculation the gas gap thickness:

$$\delta = \frac{d_p}{10}\left(1 + \frac{1}{2}|\cos\theta|\right) \tag{9}$$

Considering the gap between the cluster and the wall, the instantaneous heat transfer coefficient between the clusters and the heat exchanging surface can be obtained by the modification of Eq. (5) as

$$h_{cc_{(t<t_0)}} = \frac{1}{\frac{\delta}{k_g} + \sqrt{\frac{1.5t}{k_c\rho_c c_c}}} \tag{10}$$

Time-averaged heat transfer coefficient could be obtained by integration over the partial heat penetration period (i.e., from $t = 0$ to $t = \tau$) as following:

$$\begin{aligned}\bar{h}_{cc_{(t<t_0)}} &= \frac{1}{\tau}\int_0^{\tau} h_{cc_{(t<t_0)}}\,dt \\ &= \frac{2}{3\tau}(k_c\rho_c C_c)\left(\frac{\delta}{k_g}\right) \\ &\quad\times \ln\left[\frac{4\left(\frac{\delta}{k_g}\right)^2(k_c\rho_c C_c)}{\left(4\left(\frac{\delta}{k_g}\right)^2(k_c\rho_c C_c) - 6\tau\right)}\cdot\frac{1 - \frac{\sqrt{6}}{2\left(\frac{\delta}{k_g}\right)}\left(\frac{\tau}{k_c\rho_c C_c}\right)^{0.5}}{1 + \frac{\sqrt{6}}{2\left(\frac{\delta}{k_g}\right)}\left(\frac{\tau}{k_c\rho_c C_c}\right)^{0.5}}\right] \\ &\quad + \frac{2\sqrt{6}}{3\tau}((k_c\rho_c C_c)\tau)^{0.5}\end{aligned} \tag{11}$$

Likewise, Eq. (6) can be modified by considering the gas gap between the cluster and the wall:

$$h_{cc_{(t>t_0)}} = \frac{1}{\frac{\delta}{k_g} + \left(\frac{d_c}{k_c}\right)\left[\frac{1}{2} + \left(\frac{1}{2} + \frac{1}{Bi}\right)\left\{1 - \exp\left[-\frac{m(t-t_0)}{1+\frac{Bi}{3}}\right]\right\}\right]} \tag{12}$$

Eq. (12) may be integrated from $t = t_0$ to $t = \tau$ to give the time-averaged heat transfer coefficient over the total heat penetration period:

$$\begin{aligned}\bar{h}_{cc_{(t>t_0)}} &= \frac{\int_{t_0}^{\tau} h_{cc_{(t>t_0)}}\,dt}{\int_{t_0}^{\tau} dt} \\ &= \frac{2}{\left[C_3 + \frac{2d_c}{k_c}C_1\right]}\left\{1 - \frac{1}{C_2(\tau - t_0)}\right. \\ &\quad\left.\times \ln\left[1 + \frac{\frac{2d_c}{k_c}C_1}{C_3}(1 - \exp(C_2(\tau - t_0)))\right]\right\}\end{aligned} \tag{13}$$

where

$$C_1 = \frac{1}{2} + \frac{1}{Bi} \tag{14}$$

$$C_2 = -\frac{m}{1 + \frac{Bi}{3}} \tag{15}$$

$$C_3 = \frac{2\delta}{k_g} + \frac{d_c}{k_c} \tag{16}$$

If the contact time of the clusters is less than the total heat penetration period, Eq. (11) could be directly used to evaluate the average heat transfer coefficient:

$$\bar{h}_{cc} = \bar{h}_{cc_{(t<t_0)}} t_0 \leqslant \tau \tag{17}$$

However, when the contact time is larger than the total penetration period, both Eqs. (11) and (13) should be considered for calculating the time-averaged heat transfer coefficient. Only τ in Eq. (11) must be replaced by t_0:

Table 2
Physical and thermal properties of cluster

Property	Formula	Reference
Specific heat of cluster	$C_c = (1-\varepsilon_c)C_s + \varepsilon_c C_g$	Yusuf et al. (2005)
Density of cluster	$\rho_c = (1-\varepsilon_c)\rho_s + \varepsilon_c\rho_g$	Yusuf et al. (2005)
Thermal conductivity of cluster	$\frac{k_c}{k_g} = \varepsilon_c + \frac{(1-\varepsilon_c)}{2k_g/3k_s + 0.305(k_g/k_s)^{0.25}}$	Kunii and Smith (1960)
Cluster diameter (d_c in mm)	$\ln d_c = -1.79 + 1.555\,(U_0 - U_{mf})$	Mostoufi and Chaouki (2004)
Voidage of emulsion (cluster)	$\varepsilon_c = 1 - \frac{(1-\varepsilon_{mf})\left[0.7293 + 0.5139\left(\frac{d_p}{D_t}\right)\right]}{1+\left(\frac{d_p}{D_t}\right)}$	Saxena (1989)
Bubble fraction	$f = 0.19\left[\frac{d_p g}{U_{mf}^2\left(\frac{U_0}{U_{mf}} - A\right)^2}\right]^{-0.23}$	Kim et al. (2003)
Cluster-wall contact time	$\tau = 1.2\left[\frac{d_p g}{U_{mf}^2\left(\frac{U_0}{U_{mf}} - A\right)^2}\right]^{0.3}\left(\frac{d_p}{D_t}\right)^{0.225}$	Kim et al. (2003)

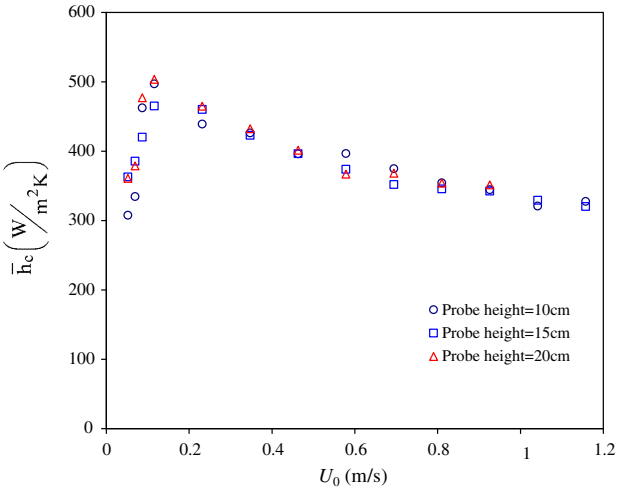

Fig. 4. Effect of superficial gas velocity for different probe locations and $d_p = 280$ μm, sand particle.

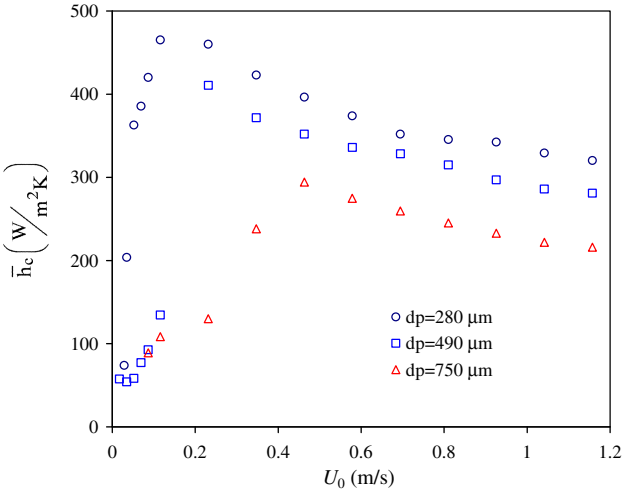

Fig. 5. Effect of particle diameter on *hc* for probe location 15 cm above the distributor.

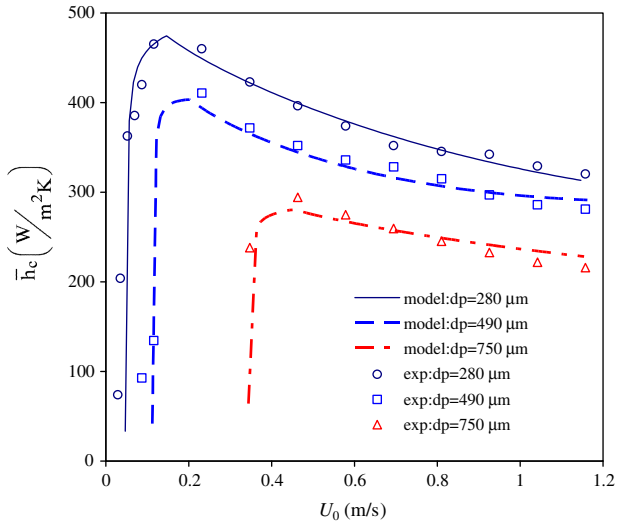

Fig. 6. Comparison of the average heat transfer coefficients obtained by the model and the experimental data from present study.

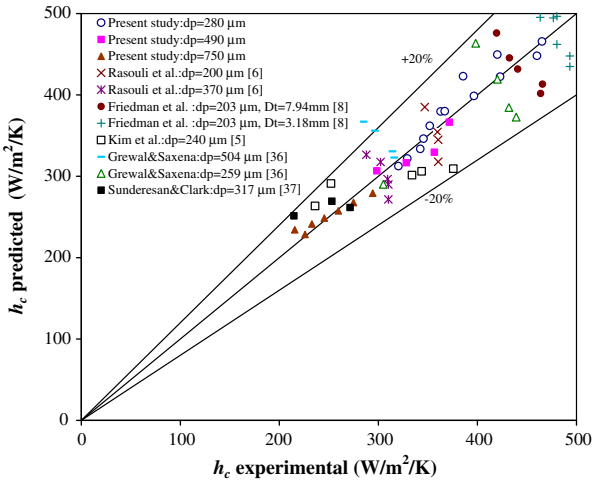

Fig. 7. Comparison of the average heat transfer coefficients obtained by the proposed model and the experimental data.

$$\bar{h}_{cc} = \left(\frac{t_0}{\tau}\right)\bar{h}_{cc_{(t<t_0)}} + \left(1-\frac{t_0}{\tau}\right)\bar{h}_{cc_{(t>t_0)}}\, t_0 > \tau \qquad (18)$$

The formulas needed for estimating the physical and thermal properties of clusters and gas are listed in Table 2.

4. Results and discussion

4.1. Experiments

In the present study, the effects of axial position of the probe in the bed, particle size and superficial gas velocity on overall heat transfer coefficient between an immersed horizontal tube and the fluidized bed were experimentally studied. The heat transfer coefficient was measured at different gas velocities in the range of packed bed conditions up to 1.2 m/s. These measurements were carried out at three different particle sizes (280, 490 and 750 μm) and three different axial positions of the probe (heights of 10, 15, 20 cm from the distributor).

Fig. 4 illustrates the variation of average heat transfer coefficient with superficial gas velocity around horizontal tube immersed in fluidized bed at different heights above the distributor. As expected, it can be seen from this figure that for the horizontally immersed tube, there is an initial increase of $\bar{h}_c$ with the superficial gas velocity. The heat transfer rate is decreased after attaining a maximum value. It can be concluded that the heat transfer rate between the tube and the fluidized bed depends on the particle concentration close to the heat transfer surface and particle residence time at the tube surface (Grewal and Saxena, 1981). The larger values of $\bar{h}_c$ could be obtained with shorter residence time of particles or clusters with higher solid holdups. The cluster residence time on the tube surface depends on the replacement rate of clusters by bubbles. Thus, the initial increase of $\bar{h}_c$ with U_0 is due to reduction in cluster residence time and further decrease is due to an increase in the bed porosity adjacent to the heat transfer surface at higher velocities. Moreover, the effect of the axial location of the horizontal tube can be seen in Fig. 4. Experiments were carried out in three different locations of the probe (10, 15 and 20 cm above the distributor). The results indicate that the overall heat transfer coefficient is independent of the axial position in the bed.

The variation of average overall convective heat transfer coefficient with particle diameter is illustrated in Fig. 5. The widely reported inverse dependency of the heat transfer coefficient to the particle size (Zabrodrky, 1966; Botterill and Desal, 1972) can be clearly observed in this figure. The trend in this figure is justified

Table 3
Discrimination of the models

Reference	Correlation	$\Sigma(\varepsilon_{iu})^2$	$\widehat{S}_i$	$\pi(M_i\,\vert Y)$
Vreedenberg (1958)	$\frac{hD_t}{k_g} = 0.66\left[\frac{GD_t(1-\varepsilon)}{\rho_g\mu\varepsilon}\right]^{0.44} Pr_g^{0.3}$	1501211	2281.37	10^{-495}
Andeen and Glicksman (1976)	$\frac{hD_t}{k_g} = 900(1-\varepsilon)\left[\left(\frac{GD_t\rho_s}{\rho_g\mu}\right)\left(\frac{\mu^2}{d_p^3\rho_g^2 g}\right)\right]^{0.326} Pr^{0.3}$	425819	647.11	10^{-138}
Petrie (1968)	$\frac{hD_t}{k_g} = 14\left(\frac{G}{G_{mf}}\right)^{1/3} pr^{1/3}\left(\frac{D_t}{d_p}\right)$	2969489	4512.7	10^{-979}
Borodulya et al. (1991)	$\frac{h_c d_p}{k_g} = 0.74Ar^{0.1}\left(\frac{\rho_s}{\rho_g}\right)^{0.14}\left(\frac{C_{ps}}{C_{pg}}\right)^{0.24}(1-\varepsilon)^{\frac{2}{3}} + 0.46Re_p Pr_g\frac{(1-\varepsilon)^{\frac{2}{3}}}{\varepsilon}$	300566	456.76	10^{-96}
Molerus and Schweinzer (1989)	$\frac{hl}{k_g} = \frac{0.125(1-\varepsilon_{mf})}{B_1\left[1+B_2(k_g/2C_{ps}\mu_g)\right]} + 0.165 pr_g^{\frac{1}{3}}\left(\frac{\rho_g}{\rho_s-\rho_g}\right)^{\frac{1}{3}}\left(\frac{1}{B_3}\right)$ $B_1 = 1 + 33.3\left[\left(\frac{U_e\rho_s C_s}{U_{mf}gk_g}\right)^{1/3} U_e\right]^{-1}$ $B_2 = 1 + 0.28(1-\varepsilon_{mf})^2 U_e U_{mf}\left(\frac{\rho_g}{\rho_s-\rho_g}\right)^{\frac{1}{2}}\left(\frac{\rho_s C_s}{gk_g}\right)^{2/3}$ $B_3 = 1 + 0.05\left(\frac{U_{mf}}{U_e}\right)$ $l = \left(\frac{\mu_g}{\rho_s-\rho_g}\right)^{\frac{2}{3}}\left(\frac{1}{g}\right)^{1/3}, U_e = U_0 - U_{mf}$	137759.8	209.35	10^{-43}
Rasouli et al. (2005)	$\frac{hD_t}{k_g} = 1.754Re_p^{0.556}Pr^{0.3}$	920571.8	1398.98	10^{-301}
Present study	If $t < t_0 \Rightarrow \bar{h}_{cc} = \bar{h}_{cc_{(t<t_0)}}$ If $t > t_0 \Rightarrow \bar{h}_{cc} = \left(\frac{t_0}{\tau}\right)\bar{h}_{cc_{(t<t_0)}} + \left(1-\frac{t_0}{\tau}\right)\bar{h}_{cc_{(t>t_0)}}$	9870.45	15.00	0.9999

by the fact that the net surface area of the particles in contact with the tube is higher for small solid particle than large particles. Another explanation could be that due to changes in the cluster motion, the cluster convection term would be higher for smaller particles.

4.2. Modeling

The experimental heat transfer coefficients as well as the corresponding predicted values from the model developed in this work are shown in Fig. 6 for the three particle sizes investigated. This figure demonstrates that there is a good agreement between the predicted values and the experimental data. This agreement over a wide range of fluidizing conditions (three particle sizes and a superficial gas velocity up to 1.2 m/s), shows the effectiveness of the proposed model. The correlation coefficient was 0.93 or higher in all cases.

The values of $\overline{h}_c$ measured in the present work and those reported in literature (Al-Busoul and Abu-Ein, 2003; Rasouli et al., 2005; Friedman et al., 2006; Grewal and Saxena, 1983; Sunderesan and Clark, 1995) are compared with the values calculated from Eq. (2) in Fig. 7. As seen in this figure, the model is able to predict the experimental heat transfer coefficient within ±20% error. Introducing more reliable correlations for parameters such as the cluster size, contact time of the cluster and gas gap thickness would further improve the predictions of the model.

In order to identify the preferred model and assess its adequacy, the statistical method of Stewart et al. (1998) was used. The results of applying this method are summarized in Table 3. As seen in this table, the model developed in this work based on the cluster renewal approach predicts the $\overline{h}_c$ values most accurately. Based on the statistical analysis of Stewart et al. (1998), the probability of this proposed model being valid exceeds 99.9% compared to other empirical correlations (Rasouli et al., 2005; Vreedenberg, 1958; Andeen and Glicksman, 1976; Petrie, 1968; Borodulya et al., 1991; Molerus and Schweinzer, 1989).

5. Conclusion

A model was developed for the evaluation of the heat transfer coefficient from fluidized beds to horizontally immersed tubes according to the cluster based approach. In this model, the particle and gas convective components of the heat transfer are considered along with the stagnant gas film, as confirmed by many investigators. Based on the experimental findings of this work and comparing the model predictions with the experimental data, it could be concluded that the proposed model predicts the $\overline{h}_c$ on a wide range of experimental conditions (gas velocity up to 1.2 m/s and three different solid particles) very well. The experimental results also showed that the heat transfer coefficient is increased with increasing the gas velocity, up to a maximum, and then declines with a slight slope, afterward. Also, the results showed that the heat transfer coefficient is inversely proportional to the solid particle diameter in the range of 280–750 μm. The probe position had minor influence on the heat transfer coefficient.

References

Al-Busoul, M., Abu-Ein, S., 2003. Local heat transfer coefficients around a horizontal heated tube immersed in a gas fluidized bed. Heat Mass Transfer 39, 355–358.

Andeen, B.R., Glicksman, L.R., 1976. Heat transfer to horizontal tubes in shallow fluidized beds. ASME Paper No. 76-HT-67, ASME AIChE Heat Transfer Conference, St. Louis, MO.

Baskakov, A.P., 1964. The mechanism of heat transfer between a fluidized bed and a surface. Int. Chem. Eng. 4, 320–324.

Baskakov, A.P., Berg, B.V., Vitt, O.K., Fillippovsky, N.F., Kirakosyan, V.A., Goldohin, J.M., Figiola, R.S., 1973. Heat transfer to objects immersed in fluidized bed. Powder Technol. 8, 273–282.

Borodulya, V., Teplitsky, Y., Sorokin, A., Markevich, I., Hassan, A., Yeryomenko, T., 1991. Heat transfer between a surface and a fluidized bed: consideration of pressure and temperature effects. Int. J. Heat Mass Transfer 34, 47–53.

Botterill, J.S.M., 1970. Heat transfer to gas-fluidized beds. Powder Technol. 4, 19–26.

Botterill, J.S.M., 1986. Fluid bed heat transfer. In: Geldart, D.. Gas Fluidization Technology. John Wiley and Sons, UK, pp. 219–258.

Botterill, J.S.M.Desal, M., 1972. Limiting factor in gas fluidized bed heat transfer. In: Powder Technol. 6, 231–238.

Cai, P., Chen, S.P., Jin, Y., Yu, Z.Q., Wang, Z.W., 1989. Effect of operating temperature and pressure on the transition from bubbling to turbulent fluidization. AIChE Symp. Ser. 85, 37–43.

Decker, N., Glicksman, L.R., 1986. Local voidage around horizontal cylinders immersed in fluidized beds. Heat and Mass Transfer in Fixed and Fluidized Beds. In: van Swaaij, W.P.M. (Ed.), Proceedings of the International Centre for Heat and Mass Transfer, vol. 20. Hemisphere Publishing Corporation, p. 95.

Friedman, J., Koundakjian, P., Naylor, D., Rosero, D., 2006. Heat transfer to small horizontal cylinders immersed in a fluidized bed. Trans. ASME, J. Heat Transfer 128, 984–988.

Gabor, J.O., 1970. Wall-to-bed heat transfer in fluidized and packed beds. AIChE Symp. Ser. 66, 76.

Gelperin, N.I., Ainshtein, V.G., Korotyanskaya, L.A., 1969. Heat transfer between a fluidized bed and staggered bundles of horizontal tubes. Int. Chem. Eng. 9, 137–142.

Glickeman, L.R., Decker, N.A., 1980. Design relationships for predicting heat transfer to tube bundles in Fluidized Bed Combustion. In: Proceedings of the Sixth Annual International Conference on Fluidized Bed Combustors, Atlanta, GA, vol. III, p. 152.

Grewal, N.S., Saxena, S.C., 1981. Maximum heat transfer coefficient between a horizontal tube and a gas–solid fluidized bed. Ind. Eng. Chem. Proc. Des. Develop. 20, 108–116.

Grewal, N.S., Saxena, S.C., 1983. Experimental studies of heat transfer between a bundle of horizontal tubes and a gas–solid fluidized bed of small particles. Ind. Eng. Chem. Proc. Des. Develop. 22, 367–376.

Horio, M., Kuroki, H., 1994. Three-dimensional flow visualization of dilutely dispersed solids in bubbling and circulating fluidized beds. Chem. Eng. Sci. 49, 2413–2421.

Huang, D., Levy, E., 2004. Gas gap at the surface of a horizontal tube in a bubbling fluidized bed. Powder Technol. 140, 131–135.

Karamavruc, A.I., Clark, N.N., 1996. A correction factor for one-dimensional heat transfer coefficients around a horizontal tube in a fluidized bed. Powder Technol. 86, 209–217.

Karimipour, S., Zarghami, R., Mostoufi, N., Sotudeh-Gharebagh, R., 2007. Evaluation of heat transfer coefficient in gas–solid fluidized beds using cluster-based approach. Powder Technol. 172, 19–26.

Khan, T., Turton, R., 1992. The measurement of instantaneous heat transfer coefficients around the circumference of a tube immersed in a high temperature fluidized bed. Int. J. Heat Mass Transfer 35, 3397–3406.

Kim, S., Ahn, J., Kim, S.D., Lee, D., 2003. Heat transfer and bubble characteristics in a fluidized bed with immersed horizontal tube bundle. Int. J. Heat Mass Transfer 46, 399–409.

Koppel, L.B., Patel, P.D., Holmes, J.T., 1970. Statistical models for surface renewal in heat and mass transfer. Part IV: wall to fluidized bed heat transfer coefficients. AICHE J. 16, 464–471.

Kubie, J., Broughton, J., 1975. A model of heat transfer in gas fluidized beds. Int. J. Heat Mass Transfer 18, 289–299.

Kunii, D., Smith, J.M., 1960. Heat transfer characteristics of porous rocks. AIChE J. 6, 71–78.

Li, H.S., Qian, R.Z., Huang, W.D., Bi, K.J., 1993. An investigation on instantaneous local heat transfer coefficients in high temperature fluidized beds – I. Experimental results. Int. J. Heat Mass Transfer 36, 4389–4395.

Mickley, H.S., Fairbanks, D.F., 1955. Mechanism of heat transfer to fluidized beds. AIChE J. 1, 374–384.

Modrak, T., 1979. Fluidized bed combustion development facility and commercial utility AFBC design assessment. Quarterly technical progress report prepared for ERPI, January through March 1979.

Molerus, O., Schweinzer, J., 1989. Prediction of gas convective part of the heat transfers to fluidized beds. In: Fan, L.S., Knowlton, T.M. (Eds.), Fluidization IV. Engineering Foundation, New York, pp. 685–693.

Mostoufi, N., Chaouki, J., 2004. Flow structure of the solids in gas–solid fluidized beds. Chem. Eng. Sci. 59, 4217–4227.

Ozkaynak, T.F., Chen, J.C., 1980. Emulsion phase residence time and its use in heat transfer models in fluidized beds. AIChE J. 26, 544–550.

Pence, D.V., Beasley, D.E., Figiola, R.S., 1994. Heat transfer and surface renewal dynamics in gas-fluidized beds. J. Heat Transfer 116, 929–937.

Petrie, J.C., 1968. In-bed heat exchangers. Chem. Eng. Prog. 64, 45–51.

Rasouli, S., Golriz, M.R., Hamidi, A.A., 2005. Effect of annular fins on heat transfer of a horizontal immersed tube in bubbling fluidized bed. Powder Technol. 154, 9–13.

Saxena, S.C., 1989. Heat transfer between immersed surfaces and gas-fluidized beds. Adv. Heat Transfer 19, 97–190.

Stewart, W.E., Shon, Y., Box, G.E.P., 1998. Discrimination and goodness of fit of multi-response mechanistic models. AIChE J. 44, 1404–1412.
Sunderesan, S.R., Clark, N.N., 1995. Local heat transfer coefficients on the circumference of a tube in a gas fluidized bed. Int. J. Multiphase Flow 21, 1003–1024.
Vreedenberg, H.A., 1958. Heat transfer between a fluidized bed and a horizontal tube. Chem. Eng. Sci. 9, 52–66.
Xavier, A.M., Davidson, J.F., 1978. Heat transfer to surfaces immersed in fluidized beds, particularly tube arrays fluidization. In: Proceedings of the Second Eng. Foundation Conf., Cambridge University Press, p. 333.
Yusuf, R., Melaaen, M., Mathisen, V., 2005. Convective heat and mass transfer modeling in gas fluidized beds. Chem. Eng. Technol. 28, 13–24.
Zabrodrky, S.S., 1966. Hydrodynamics and Heat Transfer in Fluidized Beds. M.I.T. Press, Cambridge, MA.